RSC Advances

Check for updates

Catalytic oxidation of organic pollutants in wastewater *via* a Fenton-like process under the catalysis of HNO₃-modified coal fly ash

Nannan Wang, [iD] [a] Qiang Zhao[b] and Aili Zhang*[c]

The performance of acid-modified coal fly ash (CFA) was tested for use as a catalyst of a Fenton-like process in *p*-nitrophenol (*p*-NP) wastewater treatment. The results show that HNO₃-modified coal fly ash (HFA) has a better catalytic capacity (96.6% *p*-NP removal rate) than those (<92% *p*-NP removal rate) of CFA modified by other acids (HCl, H_2SO_4, and H_3PO_4). The removal rate of the *p*-NP by the adsorption of HFA is less than 2.96%, which can be thought of as negligible compared to that removed by the catalytic oxidation process. Under the optimum experimental conditions (reaction time = 60 min, $C_{H_2O_2}$ = 170 mg L⁻¹, C_{HFA} = 10.0 g L⁻¹, pH = 2.0, mixing speed = 150 rpm, and temperature = 25 °C), a 98% *p*-NP removal rate is observed. HFA has an acute response to the change of temperature and higher temperature is welcomed (9.3% and 98% of the *p*-NP was removed at 25 and 50 °C, respectively, at 5 min). HFA can be reused 9 times with >91% of the *p*-NP removal rate, revealing an outstanding catalytic stability and reusability. The catalytic mechanism of HFA was discussed by comparing the physicochemical features of HFA with raw CFA and by proposing the reactions which occur in the Fenton-like process.

1. Introduction

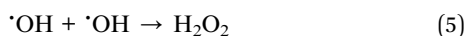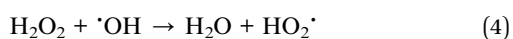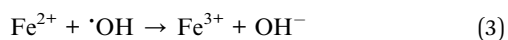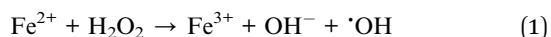In recent years, significant progress in treating refractory wastewater has been achieved by the application of advanced oxidation processes (AOPs). A common feature of AOPs is the generation of hydroxyl radicals (˙OH), which can decompose refractory organics effectively due to their strong oxidising ability (E_0 = 2.8 V). The Fenton process, as a classic AOP, can generate ˙OH *via* the reaction of Fe^{2+} with H_2O_2. The reactions that occur in the Fenton process can be described as follows:[1–3]

$$Fe^{2+} + H_2O_2 \rightarrow Fe^{3+} + OH^- + \text{˙OH} \tag{1}$$

$$Fe^{3+} + H_2O_2 \rightarrow Fe^{2+} + HO_2\text{˙} + H^+ \tag{2}$$

$$Fe^{2+} + \text{˙OH} \rightarrow Fe^{3+} + OH^- \tag{3}$$

$$H_2O_2 + \text{˙OH} \rightarrow H_2O + HO_2\text{˙} \tag{4}$$

$$\text{˙OH} + \text{˙OH} \rightarrow H_2O_2 \tag{5}$$

$$\text{˙OH} + \text{organics} \rightarrow \text{intermediates} \rightarrow \text{inorganics} \tag{6}$$

[a]*School of Mechanical Engineering, Beijing Institute of Petrochemical Technology, Beijing 102617, PR China. E-mail: wnn_flying@163.com*

[b]*Beijing BHT Environment Technology Co., Ltd, Beijing 100102, PR China*

[c]*School of Environmental Science and Technology, Dalian University of Technology, Dalian 116024, PR China. E-mail: zal58@163.com*

Although the Fenton process can oxidize a wide variety of organics, and is even be able to destroy them to produce carbon dioxide (CO_2), water (H_2O) and inorganic salts (eqn (6)), the recycling of the catalyst (Fe^{2+}) cannot be easily achieved, leading to the generation of sludge containing Fe ions. The treatment of the sludge is expensive in terms of labour, reagents, and time, and is complex in operation. Thus, exploring a novel solid catalyst that can be used in heterogeneous Fenton-like processes is necessary.

Coal fly ash (CFA) is produced from steel mills and coal-fired power plants. Over 300 billion tons of CFA is produced every year in the world.[4] Even now, CFA is still mainly treated by means of landfill, causing severe environmental pollution because of the leaching of the metallic elements that are contained in CFA. Thus, proper treatment of CFA is required. Over the years, many studies[5–14] have revealed that pre-treated CFA can be used as an effective low-cost adsorbent for the removal of organic and inorganic metallic elements (such as arsenic, nickel, calcium, copper, iron and manganese ions) in wastewater. However, the catalytic property of CFA has not attracted enough attention and just a small number of studies[15–17] have been conducted until now. Reassuringly, these studies show that the application of pre-modified CFA as a heterogeneous catalyst could have enormous potential due to the existence of transition metal oxides. The modification of CFA can be achieved by acid modification, alkali modification, and thermal modification.[18–20] However, alkali modification and thermal modification can introduce alkaline substances and destroy the space structure of CFA, respectively, which have adverse effects

on the catalytic capacity of a catalyst. Therefore, acid modification is always used to prepare the target catalyst.

The contamination of aquatic environments by chemical pollutants has been a major issue in recent years. p-Nitrophenol (p-NP) is typically one of the most refractory substances that is present in industrial wastewater, due to its high solubility and stability in water. p-NP exists in wastewater from a number of industries, such as textiles, paper and pulp, plastics etc., and is considered to be a hazardous chemical pollutant. The use of p-NP has been seriously controlled by the U.S. Environmental Protection Agency.[21] The maximum allowed concentration in water is in the range 1–20 ppb. Hence, its removal from industrial effluents is an important practical problem.

In this paper, in order to promote the application of CFA, a comprehensive study about CFA modification using HNO_3 (HFA) was conducted and its catalytic capacity was investigated by catalysing a heterogeneous Fenton-like process to degrade p-NP in wastewater. Firstly, the preparation conditions of HFA were optimized after choosing HNO_3 as the proper acid in the modification, and then the removal kinetics of p-NP in wastewater were investigated. After that, the reusability and stability of HFA were tested. Finally, the catalytic mechanism of HFA was proposed based on the investigation of (I) the effect of the HFA adsorption capacity, (II) a comparison of the chemical and physical features of HFA with those of CFA, and (III) the possible reactions that occur on the surface of HFA and in the solution.

2. Materials and methods

2.1 Chemicals and reagents

p-NP (analytical grade) was purchased from Tianjin Kermel Chemical Reagent Co., Ltd., China and was used without any further purification. The p-NP wastewater (100 mg L^{-1}) was prepared directly by diluting solid p-NP into distilled water. The hydrogen peroxide (H_2O_2) (30%, w/w), sodium hydroxide (NaOH), nitric acid (HNO_3), sulphuric acid (H_2SO_4), hydrochloric acid (HCl), and phosphoric acid (H_3PO_4) that were used in this work were of analytical grade. H_2O_2 was used directly without dilution. NaOH and different acids were dissolved and diluted, respectively, with distilled water to achieve the target concentrations. The CFA that was used was purchased from a coal-fired power plant in China (source not revealed due to a confidentiality agreement).

2.2 Preparation of HFA

Due to the existence of some impurities (such as fibers and alkaline substances) on its surface, the CFA was first washed repeatedly and adequately with distilled water before modification until the pH of the supernatant was equal to the pH value of distilled water. The loading of CFA in distilled water was 10.0 g L^{-1}. We used adequate agitation to promote the washing quality. After 12 h, the mechanical agitation was stopped and the mixture was precipitated and separated. After the washing, the washed CFA was dried at 105 °C until the weight did not change.

During the stage of modification, the washed-dried CFA was soaked in a 1 mol L^{-1} HNO_3 solution (CFA loading = 25 g L^{-1}). The mixture was stirred using a magnetic stirrer (350 rpm) for 4 h. Subsequently, the mixture was precipitated by gravity, layered, and filtered using a vacuum filter. The solid that was obtained after the filtration was dried at 105 °C until the weight stayed constant. The CFA obtained after the above processes (i.e., HFA) was stored in a drying basin for the following experiments.

2.3 Treatment procedure of p-NP wastewater

100 mL of p-NP solution (100 mg L^{-1}) with a pH pre-adjusted using NaOH and HNO_3 was prepared in a beaker (500 mL), and the temperature of the solution was controlled using a water bath. After the temperature reached the determined value (±1 °C), a certain amount of HFA was added into the solution and mixed using a mechanical agitator. The wastewater treatment started as soon as H_2O_2 was added into the beaker.

During the reaction, the mixture was sampled at specific time intervals. Meanwhile, the NaOH solution was added into the sample immediately to stop the catalytic oxidation process. All of the samples were filtrated using a vacuum pump and the filtrate was analysed to determine the concentration of the residual p-NP.

In the study of the reusability and stability of the HFA, the solid that was separated from the treated wastewater was washed using distilled water and dried until a constant weight was achieved at 105 °C. After that, the used HFA was reused again until the removal efficiency of p-NP had an obvious decrease.

For the investigation of the adsorption effect of the HFA, the adsorption isotherm was measured under fixed experimental conditions (the reaction temperature was 25 °C, the reaction time was 60 min, which is long enough to reach to the adsorption equilibrium, the pH was 2.0, the HFA loading was 10.0 g L^{-1}, and the V_{p-NP} value was 100 mL) while only the p-NP concentration changed (1, 3, 7, 10, 15, 20, 30, 40, 50, 60, 70, 80, and 90 mg L^{-1}). The maximum adsorption capacity of the HFA was obtained from the adsorption isotherm.

2.4 Characterization of HFA

The surface morphology of CFA and HFA was measured using a BET (Brunauer–Emmett–Teller) automated analyser (QUADRASORB). The analysis gas, outgas time and outgas temperature were nitrogen, 5.0 h and 300 °C, respectively.

The chemical composition of CFA and HFA was determined using X-ray fluorescence spectroscopy (XRF-1800). The maximum pipe pressure, maximum current, scanning speed, the temperature of the spectrum chamber, and power were 40 kV, 90 mA, 20° min^{-1}, 30 ± 0.1 °C, and 36 kW, respectively.

The morphology of the samples was analysed using scanning electron microscopy (SEM, JEOL, Japan) with an acceleration voltage of 15 kV and a current of 2×10^{-11} A. The ambient temperature and humidity were 16 °C and 60%, respectively.

The crystal structure of the samples was determined using X-ray diffraction (XRD) (Bruker, Germany) at room temperature with monochromatic high-intensity Cu K$_\alpha$ radiation (l = 1.5406 Å), an accelerating voltage of 40 kV and an emission current of 30 mA. The scanning range of 2θ and the scanning speed were 10–70° and 4° min^{-1}, respectively.

2.5 Analytical methods

Due to the fact that p-NP has its maximum UV-vis absorption peak at 400 nm at pH > 11 (Fig. 1), the concentration of the residual p-NP in wastewater after the treatment was measured using a UV-vis spectrophotometer (JASCO V-560, Japan) under the above conditions. The removal rate of p-NP was calculated by:

$$\text{Removal rate } (\%) = (C_0 - C_t)/C_0 \times 100\% \quad (7)$$

where C_0 and C_t are the initial and instantaneous concentrations of p-NP (mg L^{-1}).

3. Results and discussion

3.1 Effect of the acid type

Some studies[22–25] show that the acid type has an effect on the catalytic capacity of HFA. In this work, four different acids (HNO$_3$, HCl, H$_2$SO$_4$ and H$_3$PO$_4$) were chosen and tested. The results are given in Table 1. We can see that the CFA modified by H$_3$PO$_4$ has the worst performance in the catalytic degradation of p-NP (87.9% for the p-NP removal rate) while the HNO$_3$-modified CFA has the best catalytic capacity (96.6% for the p-NP removal rate). Additionally, the CFA modified by HCl and H$_2$SO$_4$ has intermediate performance.

The difference could be caused by the different ionization equilibrium constants (calculated using eqn (8) and (9)) of the acids and the corresponding calcium salt.

$$\text{HIn} \leftrightarrow \text{H}^+ + \text{In}^- \quad (8)$$

$$K_a = \frac{[\text{H}^+] \times [\text{In}^-]}{[\text{HIn}]} \quad (9)$$

H$_2$SO$_4$ molecules can ionize completely and generate H$^+$ and HSO$_4^-$. The K_a value of HSO$_4^-$ is equal to 1.02 × 10^{-2} at 25 °C
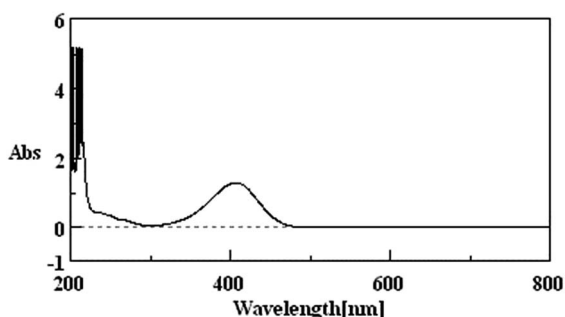

Fig. 1 The absorption curve of p-NP.

Table 1 Comparison of the degradation rates of p-NP by different acid-modified coal fly ash (T = 25 °C, pH = 2.0, $C_{H_2O_2}$ = 330 mg L^{-1}, activated CFA loading = 10 g L^{-1}, and reaction time = 40 min)

Type of HFA	Removal rate of p-NP/%
HNO$_3$-activated CFA	96.6
HCl-activated CFA	91.4
H$_2$SO$_4$-activated CFA	90.4
H$_3$PO$_4$-activated CFA	87.9

(Table 2). By comparison, H$_3$PO$_4$ ionizes partially and the three equilibrium constants (7.11 × 10^{-3}, 6.23 × 10^{-8}, and 4.50 × 10^{-13}) are much lower than those of H$_2$SO$_4$ (a strong electrolyte) and HSO$_4^-$ (a weak electrolyte). Thus, the acid modification using H$_3$PO$_4$ is weaker than that using H$_2$SO$_4$ because of the lower H$^+$ concentration in the H$_3$PO$_4$ solution.

During the H$_2$SO$_4$ modification, the generated CaSO$_4$ and Ca(HSO$_4$)$_2$ are weak electrolytes and can cover the surface of HFA. In contrast, the CaCl$_2$ and Ca(NO$_3$)$_2$ can completely dissolve in water with no possibility of covering the surface of HFA. This could be the reason that the H$_2$SO$_4$-modified CFA has a weak catalytic capacity compared to that of HNO$_3$ and HCl-modified CFA.

As for the HCl and HNO$_3$ modification, both of the two acids and the corresponding calcium salts are strong electrolytes, and the "cover effect" cannot occur. The difference in the catalytic capacity of HNO$_3$-modified and HCl-modified CFA still needs further study.

3.2 Optimization of the influencing factors on Fenton-like processes and the proposed degradation product of p-NP

Previous studies[26,27] show that the variation of the treatment time, H$_2$O$_2$ dosage, catalyst loading, wastewater pH and mixing speed have an effect on the treatment efficiency of wastewater. Therefore, they were investigated in detail in this work. Fig. 2 shows the effect of the above parameters on the removal rate of p-NP. We can see that the H$_2$O$_2$ dosage, HFA loading and mixing speed have a similar effect on the p-NP removal rate, namely, insufficient H$_2$O$_2$ dosage, HFA loading and/or mixing speed could cause the decrease of the removal rate of p-NP. The removal rate reaches a plateau when the H$_2$O$_2$ dosage, HFA loading and mixing speed reach the critical point (H$_2$O$_2$ dosage = 170 mg L^{-1}, HFA loading = 10.0 g L^{-1} and mixing speed = 150 rpm). It is economical to set the three critical points as the optimum values to achieve the best p-NP removal efficiency simultaneously.

Table 2 Ionization equilibrium constants of H$_2$SO$_4$ and H$_3$PO$_4$ at 25 °C

Type of acid	K_{a1}	K_{a2}	K_{a3}
H$_2$SO$_4$	—	1.02 × 10^{-2}	—
H$_3$PO$_4$	7.11 × 10^{-3}	6.23 × 10^{-8}	4.50 × 10^{-13}
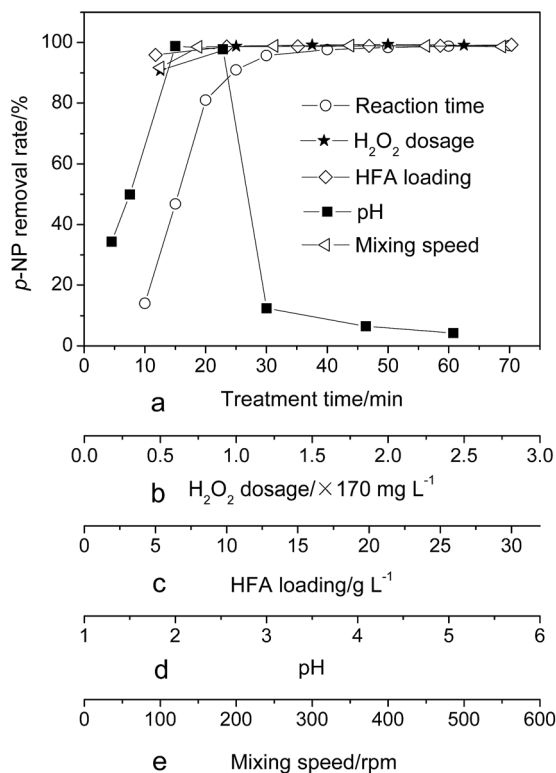
Fig. 2 Effects of the experimental parameters on the removal rate of p-NP ((a) $T = 25\ °C$, pH = 2, $C_{H_2O_2} = 170\ mg\ L^{-1}$, $C_{p\text{-}NP} = 100\ mg\ L^{-1}$ and $C_{HFA} = 10.0\ g\ L^{-1}$; (b) $T = 25\ °C$, pH = 2.0, $t = 60\ min$, $C_{p\text{-}NP} = 100\ mg\ L^{-1}$ and $C_{HFA} = 10.0\ g\ L^{-1}$; (c) $T = 25\ °C$, $C_{H_2O_2} = 170\ mg\ L^{-1}$, $t = 60\ min$, $C_{p\text{-}NP} = 100\ mg\ L^{-1}$ and pH = 2.0; (d) $T = 25\ °C$, $C_{H_2O_2} = 170\ mg\ L^{-1}$, $t = 60\ min$, $C_{p\text{-}NP} = 100\ mg\ L^{-1}$ and $C_{HFA} = 10.0\ g\ L^{-1}$; and (e) $T = 25\ °C$, pH = 2.0, $C_{H_2O_2} = 170\ mg\ L^{-1}$, $t = 60\ min$, $C_{p\text{-}NP} = 100\ mg\ L^{-1}$, and $C_{HFA} = 10.0\ g\ L^{-1}$).

The treatment time and pH have a distinct effect on the removal rate of p-NP. For the reaction time, the p-NP removal rate firstly rapidly rises and then reaches a plateau after 60 min. For the pH, the p-NP removal rate has its highest value at pH = 2, and a lower or higher pH has a negative effect on the effective treatment of wastewater.

According to the statement above, we can pick the optimum experimental conditions, *i.e.*, reaction time = 60 min, H_2O_2 dosage = 170 mg L^{-1}, HFA loading = 10.0 g L^{-1}, pH = 2.0, and mixing speed = 150 rpm. In this situation, the removal rate of p-NP is no less than 98%.

The results in some previous studies[28–30] show that the addition of an organic acid is helpful to increase the degradation of the pollutants. Because citrate and oxalate are typical in these kinds of studies,[26] the effects of citrate (0.5 mmol L^{-1}) and oxalate (0.5 mmol L^{-1}) on the removal rate of p-NP were investigated, under the optimal experimental conditions that are given above. We find that the addition of an organic acid can decrease the removal rate of p-NP from 98% (without adding the organic acid) to 71.8% (adding citrate) and 77.6% (adding oxalate). This result is different from those of some studies.[28–30]

The experimental conditions used in these cited papers[28–30] are different from ours, *i.e.*, all of the studies in the cited papers

are carried out under the irradiation of light (ultraviolet or visible light), which can obviously promote iron redox cycling by the reaction of $Fe^{III}\text{–}L + h\nu \rightarrow Fe^{II} + L^+$.[26]

In our study, we do not apply the photo-Fenton process, so the redox cycling of iron cannot occur. Instead, the active sites of HFA are occupied and a portion of the ˙OH radicals is consumed competitively by the organic acid.

The degradation product/path of p-NP has been previously investigated in some studies.[31–33] From these studies, we can find the analogous degradation path of p-NP. Hydroquinone (HQ) and 4-nitrocatechol (4-NC) can always be produced by the attack of ˙OH on the nitro-group of p-NP and the entering of ˙OH to the *ortho* position of p-NP. Meanwhile, the two products (HQ and 4-NC) can react with ˙OH to form 1,2,4-benzenetriol (1,2,4-BT).[31,32] Further reaction of 1,2,4-BT with ˙OH can generate some chain organic compounds, such as maleic acid, fumaric acid, oxalic acid and formic acid, by opening the ring.[32] These chain compounds can be oxidized further by ˙OH as well to carbon dioxide and, eventually, water.

3.3 Kinetics of p-NP degradation

The hydroxyl radical, as the strong oxidative radical, can be generated in heterogeneous Fenton-like processes and attack p-NP molecules as shown in eqn (10).

$$p\text{-NP} + OH^{\bullet} \xrightarrow{k_i} product \tag{10}$$
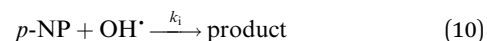
Its kinetics procedure can be characterized using:

$$-\frac{dC_{p\text{-}NP}}{dt} = k_i \times C_{˙OH} \times C_{p\text{-}NP} \tag{11}$$

where k_i is the intrinsic reaction rate constant (L mol^{-1} s^{-1}).

Assuming the concentration of ˙OH remains constant, eqn (11) becomes:

$$-\frac{dC_{p\text{-}NP}}{dt} = k_{ap} \times C_{p\text{-}NP} \tag{12}$$

Therefore,

$$\ln \frac{C_{p\text{-}NP}}{C_{0,p\text{-}NP}} = -k_{ap} \times t \tag{13}$$

where $C_{0,p\text{-}NP}$ represents the initial concentration of p-NP (mg L^{-1}), and k_{ap} is the pseudo first-order rate constant (min^{-1}), which can be determined from the slope of a $\ln \frac{C_{p\text{-}NP}}{C_{0,p\text{-}NP}}$ *versus* time graph.

3.3.1 H_2O_2 dosage. H_2O_2, as the source of ˙OH, plays an important role in heterogeneous Fenton-like processes. It was reported that a catalyst alone cannot eliminate a contaminant effectively, revealing that H_2O_2 is essential.[34] As shown in eqn (14), the molar ratio of p-NP to H_2O_2 in theory is 1 : 14, under which p-NP can be mineralized completely by H_2O_2, *i.e.*, 10 mmol L^{-1} (340 mg L^{-1}) H_2O_2 is needed for the purpose of oxidizing 0.719 mmol L^{-1} (100 mg L^{-1}) p-NP to CO_2 and H_2O completely.

$$C_6H_5NO_3 + 14H_2O_2 \rightarrow 6CO_2 + 16H_2O + HNO_3 \qquad (14)$$
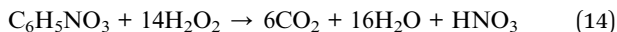
Taking the cost of treating wastewater into consideration, 340 mg L^{-1} was used as the maximum concentration and 85–340 mg L^{-1} was chosen for investigating the effect of H$_2$O$_2$. As shown in Fig. 3, the degradation of p-NP accords with the pseudo-first order kinetics and the degradation rate constant increases from 0.041 min^{-1} to 0.116 min^{-1} with the increase of H$_2$O$_2$ dosage from 85 mg L^{-1} to 340 mg L^{-1} (Table 3). In this situation, the maximum removal rate of p-NP can reach 98% within 30 min at a 340 mg L^{-1} H$_2$O$_2$ dosage.

According to the literature,[35,36] the H$_2$O$_2$ dosage should have an appropriate range. When the H$_2$O$_2$ dosage is excessive, the degradation rate of p-NP would decrease with the increase of the H$_2$O$_2$ dosage. This could be attributed to the reaction of $^•$OH with H$_2$O$_2$ and the reaction of two $^•$OH radicals (see eqn (4) and (5)). Both of the two side reactions inhibit the effective utilization of H$_2$O$_2$ and the rapid oxidation of p-NP.

When the H$_2$O$_2$ dosage is deficient (85 mg L^{-1}), the removal rate of p-NP would have an obvious decrease due to the insufficiency of the oxidizing reagent ($^•$OH). The results in this work are in good agreement with the results in the previous studies.[37–39]

3.3.2 HFA loading. The effect of HFA loading was investigated over the range from 3.0 to 20.0 g L^{-1}. The experimental results are given in Fig. 4 and Table 4. As shown in Fig. 4, the experimental data presents sound pseudo first-order kinetic behaviour. According to Table 4, the k_{ap} value increases from 0.006 to 0.236 min^{-1} over the whole range of HFA loadings. Thus, the optimal HFA loading in this work "seems" to be more than 20.0 g L^{-1}. However, before determining the "true" optimal HFA loading it is better to investigate some other factors besides comparing the k_{ap} values, such as the cost and the time of the wastewater treatment.

The experimental results in this work show that 97% of the p-NP is removed when the HFA loading is 20.0 g L^{-1} at 25 min, while 95.3% p-NP removal rate is achieved with an HFA loading of 10.0 g L^{-1} at 30 min. Within a similar reaction time approximately the same removal rate of p-NP is achieved at 10.0

Table 3 The pseudo first-order rate constants (k_{ap}) at different H$_2$O$_2$ dosages

| [H$_2$O$_2$]/mg L^{-1}	340	170	85
k_{ap}/min^{-1}	0.116	0.080	0.041

and 20.0 g L^{-1} of HFA loading. Comparing the results of those that used 10.0 g L^{-1} with those that used 20.0 g L^{-1}, the doubled loading of HFA (20.0 g L^{-1}) increased not only the usage amount of HFA, but it also doubled every factor during the preparation of HFA, including, but not limited to: the workload, working hours, and raw materials.

Thus, although increasing the HFA loading can theoretically accelerate the removal rate of p-NP, it must be controlled properly in practical applications. In this work, an HFA loading of 10.0 g L^{-1} with a degradation rate constant of p-NP of 0.138 min^{-1} is enough, and increasing the HFA loading further cannot increase the wastewater treatment efficiency obviously any more, but it does raise the treatment costs dramatically.

3.3.3 pH. The initial pH has a significant influence on the heterogeneous Fenton-like process during the treatment of organic wastewater.[40–42] Fig. 5 shows that the removal of p-NP complies with pseudo first-order kinetics behaviours according to the fitting curves of the reaction time $versus$ ln(C/C_0) (see eqn (13)). The maximum absolute value of the slope (k_{ap}) emerges at a pH of 2.0 (0.138 min^{-1}) (Table 5). At pH = 2.0, the removal rate of p-NP is 97.8% at 40 min.

When the pH is lower or higher than 2.0, the value of k_{ap} decreases sharply, $i.e.$, k_{ap} = 0.007 $versus$ pH = 1.0 and k_{ap} = 0.002 $versus$ pH = 3.0 (Table 5). In this situation, only 44% (pH = 1.0)/12.5% (pH = 3.0) of the p-NP is removed after 60 min. By comparison, controlling the pH at pH = 2.0 is better in the case of pursuing a higher removal efficiency of p-NP.

When the pH increases from 2.0, the oxidation ability of the heterogeneous Fenton-like process decreases due to deactivation of the ferrous ions. At a lower pH range (pH = 1.0), H$_2$O$_2$ could be stabilized to H$_3$O$_2^+$, as shown in eqn (15), which can decrease the production rate of $^•$OH indirectly.[43] In addition, the
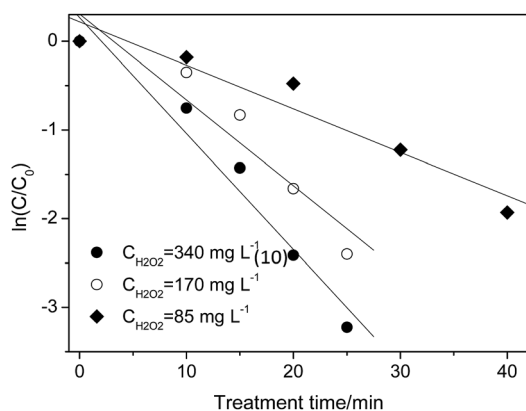
Fig. 3 Effect of H$_2$O$_2$ dosage on the p-NP degradation kinetics ($C_{p\text{-NP}}$ = 100 mg L^{-1}, T = 25 °C, C_{HFA} = 10.0 g L^{-1}, and pH = 2.0).
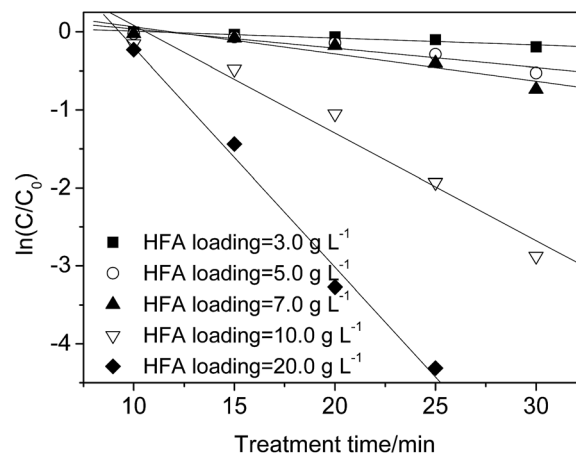
Fig. 4 Effect of HFA loading on the p-NP degradation kinetics ($C_{p\text{-NP}}$ = 100 mg L^{-1}, T = 25 °C, pH = 2.0, and $C_{H_2O_2}$ = 170 mg L^{-1}).

Table 4 The pseudo first-order degradation rate constants (k_{ap}) at different HFA loadings

HFA loading/g L^{-1}	3.0	5.0	7.0	10.0	20.0
k_{ap}/min^{-1}	0.006	0.025	0.041	0.138	0.236
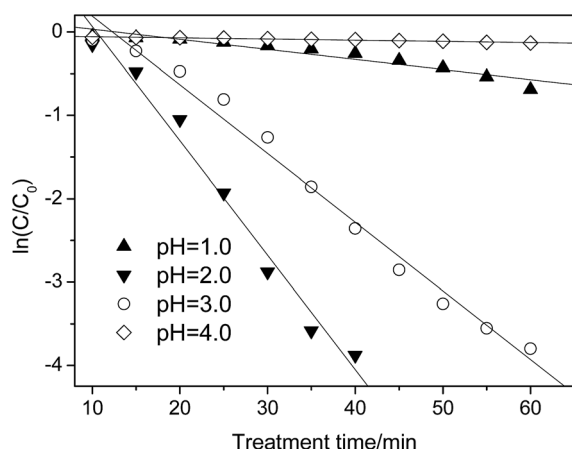
Fig. 5 Effect of pH on the p-NP degradation kinetics ($C_{p\text{-}NP}$ = 100 mg L^{-1}, $C_{H_2O_2}$ = 170 mg L^{-1}, C_{HFA} = 10.0 g L^{-1}, and T = 25 °C).

Table 5 The pseudo first-order degradation rate constants (k_{ap}) at different pH values

pH	1.0	2.0	3.0	4.0
k_{ap}/min^{-1}	0.007	0.138	0.002	—

scavenging effect of ˙OH by H^+ becomes obvious as well (eqn (16)), which decreases the effective concentration of ˙OH.[44]

$$H_2O_2 + H^+ \rightarrow H_3O_2^+ \tag{15}$$

$$\text{˙OH} + H^+ + e^- \rightarrow H_2O \tag{16}$$
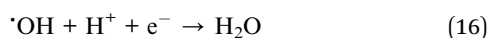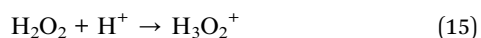
3.3.4 Temperature. The results in this work show that raising the wastewater temperature can accelerate the elimination of p-NP. 98% of the p-NP is removed at 5 min at both 50 °C and 75 °C, while only 9.3% is removed at 25 °C. It is difficult to know the residual concentration of p-NP at <5 min because the reaction time is too short to determine it exactly when relying on the current instruments. However, we can speculate that 98% of the p-NP could have been removed in less than 5 min at 75 °C.

In light of the above results, the HFA has a sensitive response to a change in temperature. This feature is beneficial for the treatment of wastewater with a higher temperature than room temperature. The determination of specific degradation kinetics of p-NP within 5 min can be realized by online detection in later work. The previous studies[45,46] considered the effect of the temperature as well, but not adequately. Considering the results in this work, a detailed study of the influence of the

temperature on the catalytic capacity of modified CFA is necessary.

3.4 Reusability and stability of HFA

For the heterogeneous Fenton-like process, evaluating the reusability and stability of the catalyst is significant for the purpose of industrial implementation because it is related to the cost of the wastewater treatment. The results in this study reveal that the pH has a remarkable effect on the dissolution of Fe due to the reaction of iron oxide on the surface of HFA with H^+ in the solution. Considering the fact that the catalytic capacity of HFA is mainly from the Fe element,[4,15] the loss/leaching of Fe from the surface of HFA will definitely affect the reusability and stability of HFA and then, inevitably, it will further affect the treatment efficiency of organic wastewater.

The reusability of the HFA was evaluated under the reaction conditions of HFA (20.0 g L^{-1}), H_2O_2 (170 mg L^{-1}), p-NP (100 mg L^{-1}), pH 2.0 and a temperature of 25 °C. The catalytic behaviour of HFA was tested in 14 consecutive experimental runs. As shown in Fig. 6, we can see that the catalytic capacity of HFA in the first nine runs does not obviously decline and the removal rate of p-NP stays >91%. From the tenth run, the catalytic capacity starts to reduce. Thus, HFA can be considered as a stable catalyst for the first nine runs of application.

We can observe that the removal rate of p-NP in Fig. 6 did not decrease significantly with the leaching of Fe into the wastewater, which could be caused by the combined action of heterogeneous and homogeneous catalysis as discussed below.

In addition, this also indicates that heterogeneous catalysis could play a more important role than homogeneous catalysis because the leached ratio of Fe became smaller and smaller with the reuse of HFA revealing that there was less and less dissolved Fe in solution with repeated usage (Table 6).

Compared to previous studies,[47–49] the modified CFA catalyst (*i.e.*, HFA) is more stable and reusable than the catalysts in other studies, which can be reused 6 times,[47] 3 times[48] and 4 times.[49]

The slow decay of the catalytic capacity of HFA contributes to the loss of active sites displayed in the form of Fe_2O_3 on the
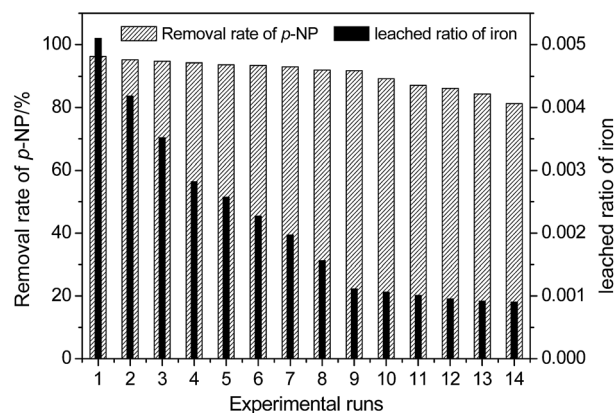
Fig. 6 Reusability and stability of the HFA catalyst for the degradation of p-NP ($C_{p\text{-}NP}$ = 100 mg L^{-1}, pH = 2.0, $C_{H_2O_2}$ = 170 mg L^{-1}, T = 25 °C, C_{HFA} = 20.0 g L^{-1}, and time = 20 min).

Table 6 The Fe^{2+} concentration in the wastewater after the treatment of p-NP wastewater in every experimental run

Experimental runs	1	2	3	4	5	6	7	8	9	10	11	12	13	14
$[Fe^{2+}]$/mg L^{-1}	0.41	0.33	0.28	0.22	0.20	0.18	0.15	0.12	0.09	0.08	0.08	0.07	0.06	0.05

surface of the HFA. As for the catalytic capacity of other metal oxides, such as Al_2O_3, these still need to be further studied individually. In this test, the leaching of Fe (right Y axis in Fig. 6) from the surface of HFA to solution causes a severe loss of active sites even though the leached ratio of iron always decreases in the consecutive experimental runs (from 0.0051 to 0.0009).

3.5 Catalytic mechanism of the HFA catalyzed Fenton-like process

3.5.1 Test of the adsorption capacity of HFA. During the treatment of p-NP wastewater, HFA can adsorb p-NP onto its surface. In order to clarify the proportion of adsorbed p-NP in the total removed amount of p-NP, an investigation of the adsorption capacity of HFA was conducted. Under fixed experimental conditions (reaction temperature = 25 °C, reaction time = 60 min, which is long enough to reach the adsorption equilibrium, pH = 2.0, HFA loading = 10.0 g L^{-1}, and $V_{p\text{-NP}}$ = 100 mL), the adsorption isotherm of p-NP (Fig. 7A) was obtained at different p-NP initial concentrations, namely, 1, 3, 7, 10, 15, 20, 30, 40, 50, 60, 70, 80, and 90 mg L^{-1}.

The line in Fig. 7B was fitted using a Langmuir model (eqn (17)):

$$m_e^{-1} = \frac{1}{K \times m_s} \times C_e^{-1} + \frac{1}{m_s} \tag{17}$$

where C_e represents the equilibrium concentration of p-NP, mg L^{-1}; m_e is the equilibrium adsorption capacity, mg g^{-1}; m_s is the adsorbed saturation concentration of p-NP on the surface of HFA, mg g^{-1}; and K is the equilibrium adsorption constant, L mg^{-1}.

We can calculate from Fig. 7B that m_s = 0.296 mg g^{-1} and K = 0.1769 L mg^{-1}. Assuming $C_{p\text{-NP}}$ = 100 mg L^{-1}, $V_{p\text{-NP}}$ = 100 mL and HFA loading = 1.0 g, under these conditions the maximum adsorption amount of p-NP by HFA is 0.296 mg in theory, accounting for 2.96% of the total amount of p-NP in the 100 mL solution. Actually, with the passage of reaction time, the p-NP concentration decreases continuously, and so the adsorption amount of p-NP cannot reach a final value of 0.296 mg. This actual amount is so little compared to the amount that was removed by oxidation that the adsorption processes can be thought of as negligible.

3.5.2 Comparison of the chemical and physical features of HFA with those of CFA. A comparison of the chemical components of HFA with those of CFA is shown in Fig. 8A. The variation of the proportions of CaO, metallic elements (especially Fe) and LOI is the primary reason causing the effective catalytic capacity of HFA compared to that of CFA.

Some studies[50–53] show that acidic conditions are appropriate in Fenton/Fenton-like processes; a higher pH could result in a remarkable reduction of the treatment efficiency of organic wastewater. Therefore, the elimination of CaO from CFA is necessary because the dissolution of CaO in water can lead to an obvious increase in the pH by generating CaOH. As shown in Fig. 8A, the proportion of CaO reduced to 1.6% (HFA) from 10.3% (CFA), indicating that the modification of CFA removed most of the CaO. This result is confirmed by the XRD results (Fig. 8B). We can see from Fig. 8B that all of the samples have peak 1 and peak 2 in their spectra, which are the peaks of quartz and mullite, respectively. However, the new and reused HFA lack peak 3, which represents CaO.

Additionally, the mass fraction of Fe_2O_3 and the LOI changed as well. As shown in Fig. 8A, the HNO_3 modification does not decrease the proportion of Fe_2O_3, but increases it (from 4.9% to 5.7%), which is helpful for increasing the catalytic capacity of the HFA. The LOI is the index of organics that are not burned completely during the burning. The carbon particles included in the LOI can cover the surface of the active sites of HFA and
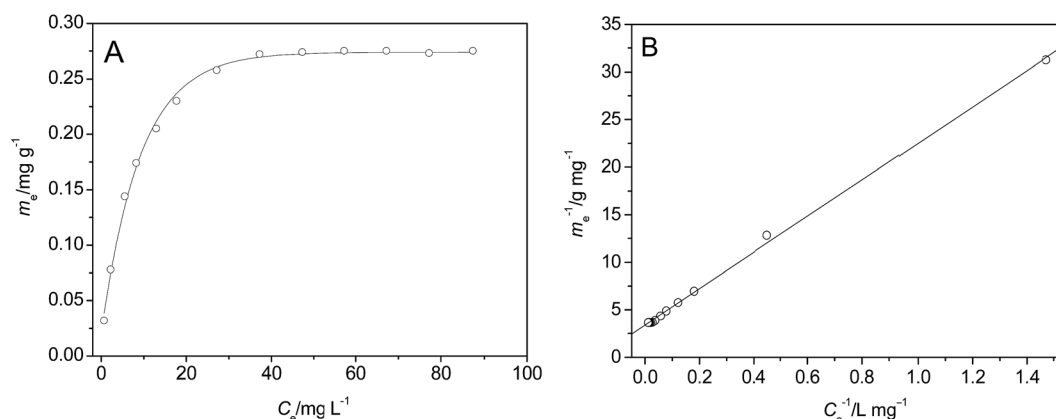
Fig. 7 Adsorption isotherms of p-NP on the surface of HFA (A) and the fitting of the data using Langmuir model (B) (T = 25 °C, t = 60 min, pH = 2.0, C_{HFA} = 10.0 g L^{-1}, and $V_{p\text{-NP}}$ = 100 mL).
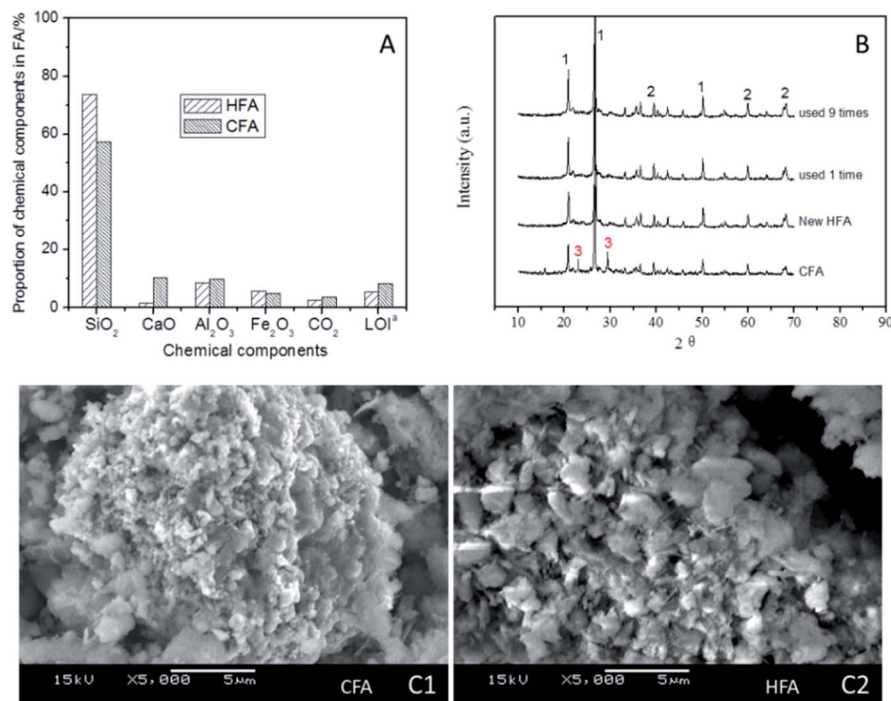
Fig. 8 Variations of physicochemical properties after CFA was modified to HFA. (A) A comparison of the chemical components of HFA and CFA ([a]: LOI means loss of ignition, it was determined after HFA and CFA were burned at 800 °C for 24 hours); (B) a comparison of XRD data for the CFA, the new HFA, the HFA that was reused 1 time and the HFA that was reused 9 times; and (C) a comparison of SEM photographs between CFA and the new HFA.
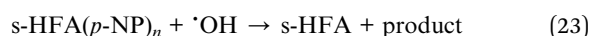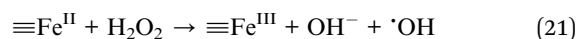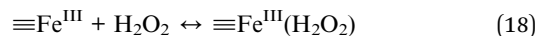
then decrease the catalytic capacity. The HNO_3 modification decreased the LOI proportion from 8.2% to 5.5%, and this actually "increases" the number of active sites by reducing the cover area of the carbon particles.

Besides the comparison of the chemical components, an investigation of the physical features of HFA and CFA was conducted as well. The results show that both the specific surface area and pore volume of CFA are increased from 11.9 m^2 g^{-1} (CFA) to 30.0 m^2 g^{-1} (HFA) and from 61.7 μL g^{-1} (CFA) to 68.0 μL g^{-1} (HFA), respectively. This result is confirmed qualitatively by the SEM images (Fig. 8C). From Fig. 8C1 we can see that the morphology of CFA is presented as a bulk structure while the HFA in Fig. 8C2 shows a honeycomb structure. This reflects the increase of the specific surface area and pore volume visually.

The above changes have important implications on the increase in the adsorption capacity and the extension of the adsorption time, which is critical to the surface catalytic oxidation of organic pollutants (see Section 3.5.3).

3.5.3   Proposed reactions occurring on the surface of HFA and in the solution. Due to the existence of active sites on the surface of HFA and dissolution of Fe from the surface of HFA, the degradation of p-NP can occur on the surface of HFA and in the solution. The reactions that occur on the surface of HFA accord with the Haber–Weiss mechanism.[54–56] The ferric ions on the surface of the HFA ($\equiv Fe^{III}$) can be reduced to ferrous ions *via* reactions (18)–(20), and then $^{\bullet}OH$ is generated subsequently on the surface of HFA through reaction (21). During the reaction, p-NP can be adsorbed on the surface of HFA (s-HFA) (eqn

(22)) and oxidized by $^{\bullet}OH$ directly (eqn (23)) without needing to spread into the solution.

$$\equiv Fe^{III} + H_2O_2 \leftrightarrow \equiv Fe^{III}(H_2O_2) \tag{18}$$

$$\equiv Fe^{III}(H_2O_2) \rightarrow \equiv Fe^{II}OOH + H^+ \tag{19}$$

$$\equiv Fe^{II}OOH \leftrightarrow \equiv Fe^{II} + HO_2^{\bullet}/O_2^{\bullet -} \tag{20}$$

$$\equiv Fe^{II} + H_2O_2 \rightarrow \equiv Fe^{III} + OH^- + {}^{\bullet}OH \tag{21}$$

$$\text{s-HFA} + p\text{-NP} \leftrightarrow \text{s-HFA}(p\text{-NP})_n \tag{22}$$

$$\text{s-HFA}(p\text{-NP})_n + {}^{\bullet}OH \rightarrow \text{s-HFA} + \text{product} \tag{23}$$

The elimination of p-NP in the solution is analogous to the homogeneous Fenton-like reaction. As shown in eqn (1), $^{\bullet}OH$ can be generated by the reaction of dissolved Fe^{2+} with H_2O_2 and p-NP can be degraded (eqn (24)) by the diffused $^{\bullet}OH$ from the surface of HFA and the generated $^{\bullet}OH$ in the solution.

$$p\text{-NP} + {}^{\bullet}OH \rightarrow \text{product} \tag{24}$$
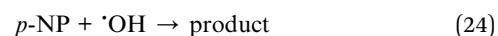
4.   Conclusions

The CFA modified by nitric acid was applied as a catalyst in a Fenton-like process and its performance was studied in p-NP wastewater treatment. The maximum adsorption amount of

HFA occupies 2.96% of the total amount of p-NP when the HFA loading is 10.0 mg L^{-1}, indicating that the adsorption can be negligible in the treatment of wastewater. Under the optimum conditions (a reaction time of 60 min, $C_{H_2O_2}$ of 170 mg L^{-1}, C_{HFA} of 10.0 g L^{-1}, pH of 2.0, and a mixing speed of 150 rpm), 98% of the p-NP was removed at room temperature. The H_2O_2 dosage and pH must be controlled at appropriate values (170 mg L^{-1} and 2.0, respectively) for avoiding the invalid decomposition/consumption of H_2O_2/$^{\bullet}OH$ and the oxidation of ferrous ions. The catalytic capacity of HFA is sensitive to the change of treatment temperature and a higher reaction temperature is helpful for simultaneously increasing the treatment efficiency and decreasing the treatment time. HFA has favourable stability and reusability, as it can be used 9 times with a >91% removal rate of p-NP. The nitric acid modification activates the CFA via increasing the Fe_2O_3 proportion, reducing the CaO and LOI proportion, and via increasing the specific surface area and pore volume. The degradation of p-NP can occur on the surface of HFA and in the solution, and the latter is similar to the homogeneous Fenton-like process.

References

1 Z. Wan and J. L. Wang, *RSC Adv.*, 2016, **105**, 103523–103531.

2 N. Flores, I. Sirés, J. A. Garrido, F. Centellas, R. M. Rodríguez, P. L. Cabot and E. Brillas, *J. Hazard. Mater.*, 2016, **319**, 3–12.

3 M. R. Carrasco-Díaz, E. Castillejos-López, A. Cerpa-Naranjo and M. L. Rojas-Cervantes, *Chem. Eng. J.*, 2016, **304**, 408–418.

4 C. Khatri and A. Rani, *Fuel*, 2008, **87**, 2886–2892.

5 K. I. Andersson, M. Eriksson and M. Norgren, *Ind. Eng. Chem. Res.*, 2011, **50**, 7733–7739.

6 A. M. Cardoso, A. Paprocki, L. S. Ferret, C. M. N. Azevedo and M. Pires, *Fuel*, 2015, **139**, 59–67.

7 M. Visa, L. Isac and A. Duta, *Appl. Surf. Sci.*, 2012, **258**, 6345–6352.

8 M. Visa, *Powder Technol.*, 2016, **294**, 338–347.

9 M. Visa and A. M. Chelaru, *Appl. Surf. Sci.*, 2014, **303**, 14–22.

10 Q. Zhou, C. J. Yan and W. J. Luo, *Mater. Des.*, 2016, **92**, 701–709.

11 P. Duan, C. J. Yan, W. Zhou and D. M. Ren, *Ceram. Int.*, 2016, **42**, 13507–13518.

12 M. Visa, L. Andronic and A. Duta, *J. Environ. Manage.*, 2015, **150**, 336–343.

13 A. M. Cardoso, M. B. Hom, L. S. Ferret, C. M. N. Azevedo and M. Pires, *J. Hazard. Mater.*, 2015, **287**, 69–77.

14 G. X. Qi, X. F. Lei, L. Li, C. Yuan, Y. L. Sun, J. B. Chen, J. Chen, Y. Wang and J. M Hao, *Chem. Eng. J.*, 2015, **279**, 777–787.

15 M. Ahmaruzzaman, *Prog. Energy Combust. Sci.*, 2010, **36**, 327–363.

16 J. B. Zhang, S. P. Li, H. Q. Li and M. M. He, *Fuel Process. Technol.*, 2016, **151**, 64–71.

17 Y. Flores, R. Flores and A. A. Gallegos, *J. Mol. Catal. A: Chem.*, 2008, **281**, 184–191.

18 C. J. An, S. Q. Yang, G. H. Huang, S. Zhao, P. Zhang and Y. Yao, *Fuel*, 2016, **165**, 264–271.

19 N. Koshy and D. N. Singh, *J. Mater. Civ. Eng.*, 2016, **28**, 04016126.

20 S. Subramanian, G. Pande, G. D. Weireld, J. M. Giraudon, J. F. Lamonier and V. S. Batra, *Ind. Crops Prod.*, 2013, **49**, 108–116.

21 M. Martin-Hernandez, J. Carrera, J. Perez and M. E. Suarez-Ojeda, *Water Res.*, 2009, **43**, 3871–3883.

22 K. Huang, K. Inoue, H. Harada, H. Kawakita and K. Ohto, *Trans. Nonferrous Met. Soc. China*, 2011, **21**, 1422–1427.

23 F. Pacheco-Torgal and S. Jalali, *Construct. Build. Mater.*, 2009, **23**, 3485–3491.

24 M. I. Muñoz, A. J. Aller and D. Littlejohn, *Mater. Chem. Phys.*, 2014, **143**, 1469–1480.

25 B. A. Labaran and M. S. Vohra, *Desalin. Water Treat.*, 2016, **57**, 16034–16052.

26 N. N. Wang, T. Zheng, G. S. Zhang and P. Wang, *J. Environ. Chem. Eng.*, 2016, **4**, 762–787.

27 N. N. Wang, T. Zheng, J. P. Jiang and P. Wang, *Chem. Eng. J.*, 2015, **260**, 386–392.

28 Y. Baba, T. Yatagai, T. Harada and Y. Kawase, *Chem. Eng. J.*, 2015, **277**, 229–241.

29 S.-Q. Liu, L.-R. Feng, N. Xu, Z.-G. Chen and X.-M. Wang, *Chem. Eng. J.*, 2012, **203**, 432–439.

30 P. A. Soares, M. Batalha, S. M. A. G. U. Souza, R. A. R. Boaventura and V. J. P. Vilar, *J. Environ. Manage.*, 2015, **152**, 120–131.

31 N. Daneshvar, M. A. Behnajady and Y. Z. Asghar, *J. Hazard. Mater.*, 2007, **139**, 275–279.

32 S.-P. Sun and A. T. Lemley, *J. Mol. Catal. A: Chem.*, 2011, **349**, 71–79.

33 D. Wan, W. B. Li, G. H. Wang, L. L. Lu and X. B. Wei, *Sci. Total Environ.*, 2017, **574**, 1326–1334.

34 P. F. Collins, H. Diehl and G. F. Smith, *Anal. Chem.*, 1959, **31**, 1862–1867.

35 H. F. Zhang, X. T. Hong, S. D. Shan and X. L. Yuan, *RSC Adv.*, 2016, **97**, 95129–95136.

36 Y. H. Wang, C. J. Feng, Y. Li, J. Y. Gao and C. P. Yu, *Chem. Eng. J.*, 2017, **307**, 679–686.

37 Z. Wan and J. L. Wang, *J. Hazard. Mater.*, 2017, **324**, 653–664.

38 B. Kakavandi and A. A. Babaei, *RSC Adv.*, 2016, **88**, 84999–85011.

39 S. H. Chen and D. Y. Du, *J. Cent. South Univ.*, 2014, **21**, 1448–1452.

40 A. L. Zhang, N. N. Wang, J. T. Zhou, P. Jiang and G. F. Liu, *J. Hazard. Mater.*, 2012, **201–202**, 68–73.

41 N. Li, P. Wang, C. Zuo, H. L. Cao and Q. S. Liu, *Environ. Eng. Sci.*, 2010, **27**, 271–280.

42 N. N. Wang, T. Zheng, J. P. Jiang, W. S. Lung, X. J. Miao and P. Wang, *Chem. Eng. J.*, 2014, **239**, 351–359.

43 B. G. Kwon, D. S. Lee, N. Kang and J. Yoon, *Water Res.*, 1999, **33**, 2110–2118.

44 X. J. Ma and H. L. Xia, *J. Hazard. Mater.*, 2009, **162**, 386–390.

45 E. Saputra, S. Muhammad, H. Q. Sun, H. M. Ang, M. O. Tade and S. B. Wang, *Catal. Today*, 2012, **190**, 68–72.

46 M. R. Becelic-Tomin, M. B. Dalmacija, B. D. Dalmacija, L. M. Rajic and D. D. Tomasevic, *Hem. Ind.*, 2012, **66**, 485–494.

47 G. Q. Gan, J. Liu, Z. X. Zhu, Z. Yang, C. L. Zhang and X. H. Hou, *Chemosphere*, 2017, **168**, 254–263.

48 M. R. Carrasco-Díaz, E. Castillejos-López, A. Cerpa-Naranjo and M. L. Rojas-Cervantes, *Chem. Eng. J.*, 2016, **304**, 408–418.

49 J. J. Zhang, X. H. Zhang and Y. F. Wang, *RSC Adv.*, 2016, **16**, 13168–13176.

50 M. Usman, K. Hanna and S. Haderlein, *Sci. Total Environ.*, 2016, **569**, 179–790.

51 W. Q. Pan, G. S. Zhang, T. Zheng and P. Wang, *RSC Adv.*, 2015, **5**, 27043–27051.

52 M. Hartmann, S. Kullmann and H. Keller, *J. Mater. Chem.*, 2010, **20**, 9002–9017.

53 M. Moussavi and S. Matavos-Aramyan, *Korean J. Chem. Eng.*, 2016, **33**, 2384–2391.

54 L. Gu, N. W. Zhu and P. Zhou, *Bioresour. Technol.*, 2012, **118**, 638–642.

55 I. S. X. Pinto, P. H. V. V. Pacheco, J. V. Coelho, E. Lorenc, J. D. Ardisson, J. D. Fabris, P. P. de Souza, K. W. H. Krambrock, L. C. A. Oliveira and M. C. Pereira, *Appl. Catal., B*, 2012, **119–120**, 175–182.

56 R. C. C. Costa, F. C. C. Moura, J. D. Ardisson, J. D. Fabris and R. M. Lago, *Appl. Catal., B*, 2008, **83**, 131–139.

This journal is © The Royal Society of Chemistry 2017